iJRASET
International Journal For Research in Applied Science and Engineering Technology

# INTERNATIONAL JOURNAL FOR RESEARCH

IN APPLIED SCIENCE & ENGINEERING TECHNOLOGY

**Volume:** 9 **Issue:** XII **Month of publication:** December 2021

**DOI:** https://doi.org/10.22214/ijraset.2021.39539

www.ijraset.com

Call: 08813907089 | E-mail ID: ijraset@gmail.com

International Journal for Research in Applied Science & Engineering Technology (IJRASET)
*ISSN: 2321-9653; IC Value: 45.98; SJ Impact Factor: 7.538*
*Volume 9 Issue XII Dec 2021- Available at www.ijraset.com*

# Simulation of Fibre Bragg Grating as Strain Sensor for Property Intrusion

Muhammad Arif Bin Jalil
*Department of Physics, Faculty of Science, Universiti Teknologi Malaysia, 81310 Johor Bahru, Johor, Malaysia*

***Abstract:*** ***This study will demonstrate a strain sensor based on the optical Fibre Bragg Grating (FBG) sensing technology as it is known to have stable and reliable wavelength and response as function of the applied strain. This kind of sensor can perform accurate measurements of small ground vibration and monitor seismic activity thanks to their high sensitivity to dynamic strains induced by acceleration variation which can use to prevent property intrusion or burglary. To understand the FBG sensor more, few of its characteristics such as strain, spectral reflectivity and bandwidth and their connection with the fibre grating length and refractive index is being studied.***

***Keywords: Fibre Bragg Grating(FBG); strain sensor; strain; spectral reflectivity; bandwidth; fibre grating length; refractive index; safety; property intrusion.***

## I. INTRODUCTION

The optical Fibre Bragg Grating (FBG) was first demonstrated by Hill et al. in 1978 where the discovery of its photosensitivity is discovered. By introducing periodic changes in the refractive index profile of the fibre core, FBGs can be formed in the fibre core. The resonance or Bragg wavelength ($\lambda_B$) of FBG is

$$\lambda_B = 2n_{\text{eff}}\Lambda \quad [1]$$

Where $\Lambda$ is the periodicity (pitch) of the grating, and $n_{eff}$ is the effective refractive index of the core. The shifts in Bragg wavelength are due to the applied strain($\varepsilon$) and temperature changes(T) which is

$$\frac{\Delta\lambda_B}{\lambda_B} = K_\varepsilon \varepsilon + K_T T \quad [2]$$

The physical elongation of the grating pitch and strain-optic coefficient of the fibre will determine the strain effect on the fibre and hence the coefficient, K$\varepsilon$.

When the FBG sensor is installed on the surface of the mechanical structure or embedded in the mechanical structure, the K$\varepsilon$ and KT values are different from those of the bare fibre. They are affected by and usually determined by the mechanical and thermal properties of the structural material and the properties of the fibre protective coating, and the material used to bond the fibre to the structure [3]. There are many papers that discuss the various aspects of FBG sensor technology which are by Kersey et al. [4], Othonos and Kalli [5], and Lau [6].

Fibre optic sensor technology has been exploited by the research community over the past the past two decades and still actively being explore because of its relatively simple design, low power consumption and relatively low maintenance cost, and therefore the flexibility it offers for both commercial and military applications [7][8]. Other than that, as the FBG technology sensor have been widely used, many improvements have been done especially on the measurement accuracy of FBG sensor arrays where multiple gas absorption lines are used as the absolute reference [9-13] and by using multiple signal processing techniques to enhance the output signal and mixing multipoint FBG sensor systems [14][15].

This study will demonstrate a strain sensor based on the optical FBG sensing technology as it is known to have stable and reliable wavelength and response as function of the applied strain. This kind of sensor can perform accurate measurements of small ground vibration and monitor seismic activity thanks to their high sensitivity to dynamic strains induced by acceleration variation [16][17].

FBG sensors require no electrical power in the sensor head as they transfer signals that are all optical which is confined in the optical cables and intrinsically immune to electromagnetic interference [18][19]. These characteristics makes it more favorable. Furthermore, fibre optic Bragg grating sensors are lightweight and compact. The typical sizes are only several centimeters long and 125µm in diameter. As it has a small size, multiple FBGs which is usually more than 20 can be monitored in one single optical fibre. Additional to that, special interrogator techniques are done where it allows for more than 1000 FBG sensors to be available on a single fibre. FBGs also exhibit a good corrosion resistance. These advantages are very useful and crucial to ensure that the sensor can be implanted underground or other bad conditions [20][21].

 

## II. METHODOLOGY

These are the methods, parameters and techniques used in this study to obtain required data and results. This framework is based on simulation by using the software MATLAB which can simulate the optical sensor.

### A. System Design

The main components used for this FBG design are :

1) Parameters used for simulation of FBG designs are effective refractive index ($neff$), Bragg wavelength ($\lambda_B$), grating period ($\Lambda$) and the strain optic constant ($\rho e$).
2) Using the single mode fibre with core cladding of diameter ratio 9/125 μm.
3) Measuring the shift in Bragg wavelength using the Optical Spectrum Analyser (OSA).

### B. Simulation Tools

GNU Octave (GUI) which is an open source that develop is used in running the simulation such as MATLAB software of version R2021a has been used. By declaring the theoretical expression and identified parameters, MATLAB software will be able to generate a mathematical operation where data and graphs are obtained.

### C. Parameters Setting

Table below shows the details of main parameters that is used in this simulation. These parameters will help to show how the sensor will behave or react upon sensing changes due to the changes in strain.

Table 1 Parameter and values used in simulation

| Parameters | Values |
|---|---|
| Effective refractive index ($n_{eff}$) | 1.46 |
| Bragg wavelength ($\lambda_B$) | 1550nm |
| Grating period ($\Lambda$) | 530nm |
| Strain optic constant ($p_e$) | 0.22 |

### D. Formulas Identification

1) *Strain*

$$\varepsilon = \frac{\Delta l}{l}$$

The change of length of the fibre will calculated using the above equation. The changes of fibre length used for the calculation is from 0.000 mm to 0.550 mm with the increment of 0.050 mm.

2) *Bragg Wavelength Shift*

$$\Delta\lambda_B = \lambda_B(1 - p_e)\varepsilon$$

$\Delta\lambda_B$ is the Bragg wavelength shift, $\lambda_B$ is Bragg wavelength, $\varepsilon$ is the strain of the grating and $pe$ is the effective strain-optic constant which is fixed at 0.22. For every strain, the Bragg wavelength is assumed to incrementally increase at 0.20 nm ranging from 1549.40 nm to 1551.60 nm.

*3) Spectral Reflectivity*

The spectral reflectivity is calculated using the following equation.

$$R(L,\lambda) = \tanh^2(\gamma L)$$

The grating length used for the simulation is set to L=2, 4, 6, 8 and 10 mm. While for the refractive index $\Delta n$ = 0.0003, 0.0005, 0.0008, 0.0012, 0.0015 and 0.0020 is used.

*4) Bandwidth*

The bandwidth for a uniform FBG is expressed as:

$$\Delta\lambda = \frac{{\lambda_B}^2}{n_{eff}\pi L}\sqrt{\pi^2 + (\kappa L)^2}$$

Where $\Delta\lambda$ is the bandwidth of FBG, $\lambda_B$ is Bragg wavelength, $n_{eff}$ is effective refractive index, L is the length of FBG and $\kappa$ is coupling coefficient. Same as in 2.4.3, the values used for grating length,L and refractive index $\Delta n$ remains unchanged.

## III. RESULTS AND DISCUSSION

This simulation demonstrates the FBG characteristics of a strain sensor. When strain is applied, the Bragg wavelength experience changes to it. Other than that, the reflectivity, and the bandwidth of FBG is also affected when there are differences in the grating length, Δl and the refractive index, Δn. The result of the simulation is shown in Table 2 until Table 4.

*A.*

*1) Strain Measurement*

Table 2 Applied strain due to changes in fibre length

| **Δ*l* (±0.05mm)** | **Strain (με)** |
|---|---|
| 0.000 | 0.000 |
| 0.050 | 1111.11 |
| 0.100 | 2222.22 |
| 0.150 | 3333.33 |
| 0.200 | 4444.44 |
| 0.250 | 5555.56 |
| 0.300 | 6666.67 |
| 0.350 | 7777.78 |
| 0.400 | 8888.89 |
| 0.450 | 10000.00 |
| 0.500 | 11111.10 |
| 0.550 | 12222.20 |

As shown in Table 3.1, the strain measured changes due to the difference in length of fibre. The strain measured increase as the change of fibre length increases. When the fibre is at its original length, the strain measured is zero. However, when the length changes increase by 0.550mm, the strain measured is 12222.20 με.

*2) Bragg Wavelength Shift*

Table 3 Shift in Bragg wavelength due to applied strain

| Strain (με) | Bragg wavelength,$\lambda_B$ (±0.10nm) | Bragg wavelength shift, $\Delta\lambda_B$ (±0.10nm) |
|---|---|---|
| 0.000 | 1549.40 | 0.00 |
| 1111.11 | 1549.60 | 1.34 |
| 2222.22 | 1549.80 | 2.67 |
| 3333.33 | 1550.00 | 4.03 |
| 4444.44 | 1550.20 | 5.37 |
| 5555.56 | 1550.40 | 6.72 |
| 6666.67 | 1550.60 | 8.06 |
| 7777.78 | 1550.80 | 9.41 |
| 8888.89 | 1551.00 | 10.75 |
| 10000.00 | 1551.20 | 12.10 |
| 11111.10 | 1551.40 | 13.45 |
| 12222.20 | 1551.60 | 14.79 |

It is shown that the Bragg wavelength shift increase as the strain applied increase. It shifted to 14.79nm when 12222.20 με is applied.

*3) Spectral Reflectivity*

Table 4 shows the spectral reflectivity dependency with the fibre grating length and the change in refractive index.

Table 4 Shift in Bragg wavelength due to applied strain

| Grating length,L (mm) | Δn = 0.0003 | Δn = 0.0005 | Δn = 0.0008 | Δn = 0.0012 | Δn = 0.0015 | Δn = 0.0020 |
|---|---|---|---|---|---|---|
| | R (%) | | | | | |
| 2.0 | 59.78 | 79.42 | 92.76 | 98.48 | 99.55 | 100 |
| 4.0 | 94.60 | 99.98 | 99.98 | 100 | 100 | 100 |
| 6.0 | 99.50 | 99.98 | 100 | 100 | 100 | 100 |
| 8.0 | 99.96 | 99.99 | 100 | 100 | 100 | 100 |
| 10.0 | 99.99 | 99.99 | 100 | 100 | 100 | 100 |

*4) Bandwidth:* The data shows that the bandwidth values with differ with the grating lengths. As the grating length increase, the bandwidth will decrease. For when $\Delta n$ = 0.0005, when L=2.0 mm, the bandwidth is 1.16nm. As the L increases to 10.0 mm, the new bandwidth is 0.26.

Table 5 Changes in bandwidth due to grating length and refractive index changes

| Grating length,L (mm) | Δn = 0.0003 | Δn = 0.0005 | Δn = 0.0008 | Δn = 0.0012 | Δn = 0.0015 | Δn = 0.0020 |
|---|---|---|---|---|---|---|
| | Bandwidth(nm) | | | | | |
| 2.0 | 1.16 | 1.25 | 1.43 | 1.74 | 2.01 | 2.44 |
| 4.0 | 0.55 | 0.70 | 0.96 | 1.36 | 1.66 | 2.17 |
| 6.0 | 0.43 | 0.61 | 0.90 | 1.31 | 1.62 | 2.15 |
| 8.0 | 0.38 | 0.57 | 0.88 | 1.29 | 1.61 | 2.13 |
| 10.0 | 0.26 | 0.55 | 0.87 | 1.28 | 1.60 | 2.12 |

*B.*

*1) Bragg Wavelength Shift*

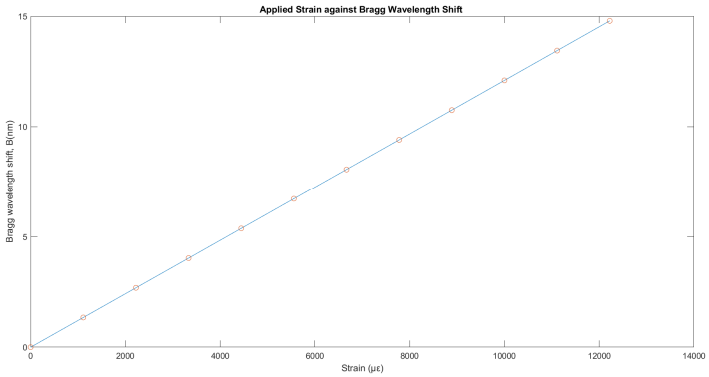


Figure 1 Graph of applied strain against Bragg wavelength shift

Figure 1 shows the relationship between the applied strain and the Bragg wavelength shift. As shown in the figure, the variables are directly proportional to each other. It is shown that the Bragg wavelength shift increase as the strain applied increase. It shifted to 14.79nm when 12222.20 με is applied.

*2) Spectral Reflectivity Dependence On Refractive Index Change*

A graph of spectral reflectivity of FBG with different refractive index change is plotted based on the data obtained in Table 4.

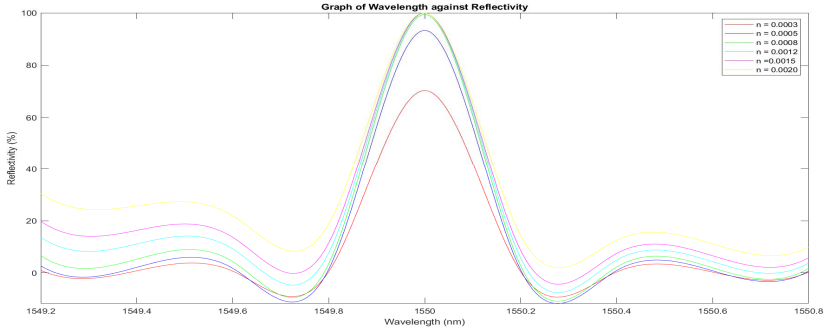


Figure 2 The reflection spectrum of FBG with various reflective index change at grating length of *L* = 2mm

It is shown that as refractive index changes increase, the reflectivity increases too. It increases to 100% with $\Delta n$ = 0.0020 when the grating length was 2.0 mm.

*3) Spectral Reflectivity Dependence On Grating Length*

Graph of spectral reflectivity of FBG for different grating length is plotted as shown in Figure 3.

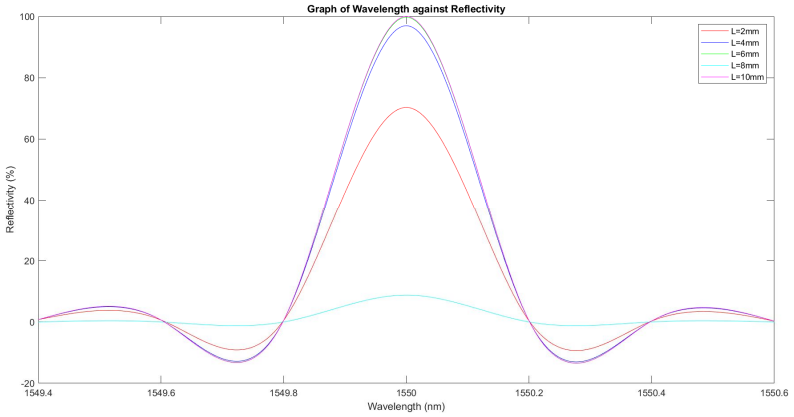


Figure 3 The reflection spectrum of FBG for various grating length at reflective index change of $\Delta n$ = 0.0003

It is shown that reflectivity of FBG changes with different grating length when the refractive index changes is fixed at $\Delta n$ = 0.0003 The reflectivity is at 59.78% when the grating length L is at 2.0mm. However, at L=10.0mm, the reflectivity increases until 99.99%.

*4) Bandwidth*

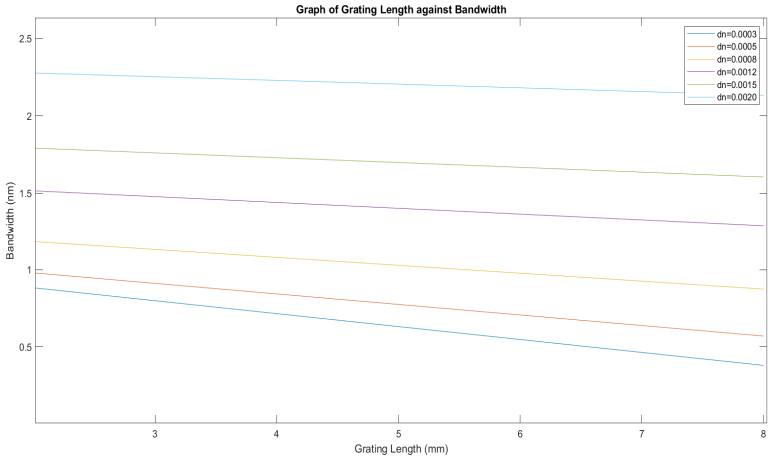


Figure 4 Relationship between FBG bandwidth and grating length with different refractive index

## IV. CONCLUSIONS

The study is to propose the applicationS of FBG using strain sensor in detecting for intrusion in private properties with the help of MATLAB software for the simulation. It also aims to bring new technique for other researchers in analyzing the characteristics without limiting the simulation techniques that can be implemented.

The results obtained in this study is similar to the previous studies. By using simulation, FBG characteristics can easily be analyzed. Characteristics such as the strain, spectral reflectivity and bandwidth and their connection with the fibre grating length and refractive index have been successfully analyzed.

Based on what is obtained from the simulation, strain is available when there are changes to length of the fibre. As the strain increase, the Bragg wavelength shift increases too. Hence, as the length increase, the reflectivity of FBG increase too which also cause the refractive index to increase. As for the bandwidth, it will decrease as the grating length and refractive index increase.

## V. ACKNOWLEDGEMENTS

The author would like to thank the Ministry of Higher Education of Malaysia (MOHE) and Universiti Teknologi Malaysia, UTM for providing GUP (2020/2021) grants in order to conduct this research and developing the paper. The author report no conflicts of interest in this work.

## REFERENCES

[1] Hill, K. O., Fujii, Y., Johnson, D. C., & Kawasaki, B. S. (1978). Photosensitivity in optical fibre waveguides: Application to reflection filter fabrication. Applied Physics Letters, 32(10), 647–649.
[2] Department of Electrical Engineering, The Hong Kong Polytechnic University, Hong Kong, & Jin, W. (2007). Structural Strain and Temperature Measurements Using Fibre Bragg Grating Sensors.
[3] Yuan, L., & Yang, J. (2003). Multiplexed Mach–Zehnder and Fizeau tandem white light interferometric fibre optic strain/temperature sensing system. Sensors and Actuators A: Physical, 105(1), 40–46.
[4] A. D. Kersey, M. A. Davis, H. J. Patric, M. LeBlanc, K. P. Koo, C. G. Askins, M. A. Putnam, and E. J. Friebele, "Fibre grating sensors," J. Lightwave Technol., 15, 1442-1462 (1997)
[5] A. Othonos and K. Kalli, "Fibre Bragg Gratings: Fundamentals and Applications in Telecommunications and Sensing," Artech House, Norwood, pp. 301-396, (1999)
[6] K. T. Lau, "Fibre-optic sensors and smart composites for concrete applications," Mag. Concrete Res., 55, 19-34 (2003).
[7] Laudati, A., Mennella, F., Giordano, M., D'Altrui, G., Calisti Tassini, C., & Cusano, A. (2007). A Fibre-Optic Bragg Grating Seismic Sensor. IEEE Photonics Technology Letters, 19(24), 1991–1993
[8] Yin, S., Ruffin, P. B., & Yu, F. T. S. (2017). Fibre Optic Sensors, Second Edition (2nd ed.). Amsterdam University Press.
[9] SpillmanJr, W. B., Mayer, M., Bennett, J., Gong, J., Meissner, K. E., Davis, B., Claus, R. O., Muelenaer Jr, A. A., & Xu, X. (2004). A smart bed for non-intrusive monitoring of patient physiological factors. Measurement Science and Technology, 15(8), 1614–1620.
[10] Allwood, G.A.; Wild, G.; Hinckley, S.. Fibre optic acoustic sensing for intrusion detection systems. In Proceedings of ACOUSTICS, Gold Coast, Australia, 2–4 November. 2011
[11] Cusano, A.; Laudati, A.; Iele, A.; Bruno, F.A.; Parente, G.; Giordano, M.; Mazzino, N.; Bocchetti, G. Smart Railways in Italy. Proceedings of the 3th Asia Pacific Workshop on Structural Health Monitoring APWSHM, Tokyo, Japan, 30 November–2 December 2010.
[12] Laudati, A.; Mennella, F.; Esposito, M.; Cusano, A.; Cutolo, A.; Giordano, M.; Campopiano, S. Railway Monitoring by Fibre Bragg Grating Sensors. Proceedings of the Third European Workshop on Optical Fibre Sensors, Naples, Italy, 4–6 July 2007.
[13] Laudati, A.; Lanza, G.; Cusano, A.; Cutolo, A.; Breglio, G.; Giordano, M.; Antonelli, A. Railway Monitoring and Train Tracking by Fibre Bragg Grating Sensors: A Case Study in Italy. Proceedings of the 4th European Workshop on Structural Health monitoring EWSHM, Krakow, Poland, 2–4 July 2008.
[14] C. C. Chan, W. Jin, H. L. Ho, D. N. Wang, and Y. Wang, "Improvement of measurement accuracy of fibre Bragg grating sensor systems by use of gas absorption lines as multi-wavelength references," Electron. Lett., 37, 742-743 (2001).
[15] W. Jin, C. C. Chan, and H. L. Ho, "Fibre Bragg grating sensors," Chinese patent no. ZL0120900.X, (2003).
[16] C. C. Chan, C. Z. Shi, J. M. Gong, and W. Jin, "Enhancement of the measurement range of FBG sensors in a WDM network using a minimum variance shift technique coupled with amplitude wavelength dual coding," Opt. Comrnun., 215, 289-294 (2003).
[17] C. Z. Shi, C. C. Chan, and W. Jin, "Improving the performance of a FBG sensor network using a genetic algorithm," Sensor. Actuat. A Phys., 107, 57-61 (2003)
[18] C. C. Chan, C. Z. Shi, and W. Jin, "Improving the wavelength detection accuracy of FBG sensors using an ADALINE network," IEEE Photon. Tech., 15, 1126-1128 03).
[19] Dorleus, J.; Zhang, Y.; Ning, J.; Koscica, T.; Li, H.; Cui, H.L.(2009). A Fibre Optic Seismic Sensor for Unattended Ground Sensing Applications. ITEA J. , 30, 455–460.
[20] Division of Security Policy, Office of Nuclear Security, and Incident Response(2011). In Intrusion Detection Systems and Subsystems; Office of Nuclear Security and Incident Response: Washington, DC, USA; March.
[21] Othonos, A., Kalli, K., Pureur, D., & Mugnier, A. (2006). Fibre Bragg Gratings. Springer Series in Optical Sciences, 189–269.
[22] Dass, R. A. S. D. R. A. S. (2019, November 9). Crime Trends and Patterns in Malaysia | Kyoto Review of Southeast Asia. Kyoto Review of Southeast Asia | Promoting Exchange among the Intellectual Communities of Southeast Asia, We Bring News of Publications, Debates and Ideas, through Lively and Accessible Writing. https://kyotoreview.org/trendsetters/crime-trends-and-patterns-in-malaysia/
[23] ISHAK, S. U. R. Y. A. T. I. (2016). THE COSTS OF CRIME TO THE SOCIETY IN MALAYSIA, 11(3). https://www.ijbel.com/wp-content/uploads/2017/01/ECON-136.pdf
[24] Wild, G., & Hinckley, S. (2011). A Fibre Bragg Grating Sensor as a Receiver for Acoustic Communications Signals. Sensors, 11(1), 455–471.
[25] Doyle, C. (2003). Fibre Bragg Grating Sensors: An Introduction to Bragg Gratings and Interrogation Techniques.
[26] Wang, J., Liu, T., Song, G., Xie, H., Li, L., Deng, X., & Gong, Z. (2014). Fibre Bragg grating (FBG) sensors used in coal mines. Photonic Sensors, 4(2), 120–124.
[27] Zhang, Y., Li, S., Yin, Z., Pastore, Jr., R., O'Donnell, K., Pellicano, M., Kosinski, J., & Cui, H.-L. (2005). Fibre Bragg grating sensors for seismic wave detection. 17th International Conference on Optical Fibre Sensors.
[28] Kheirkhah Sangdeh, P., & Zeng, H. (2019). Overview of Multiplexing Techniques in Wireless Networks. Multiplexing. https://doi.org/10.5772/intechopen.85755
[29] N'cho, J. S., & Fofana, I. (2020). Review of Fibre Optic Diagnostic Techniques for Power Transformers. Energies, 13(7), 1789. https://doi.org/10.3390/en1307178
[30] Zhang, W., Zhang, M., Wang, X., Zhao, Y., Jin, B., & Dai, W. (2019). The Analysis of FBG Central Wavelength Variation with Crack Propagation Based on a Self-Adaptive Multi-Peak Detection Algorithm. Sensors, 19(5), 1056. https://doi.org/10.3390/s19051056
[31] Meggitt, B.T. Fibre optics in sensor instrumentation. In Instrumentation Reference Book, 4th ed.; Boyes, W., Ed.; Butterworth-Heinemann/Elsevier: Oxford, UK, 2010; pp. 191–216.

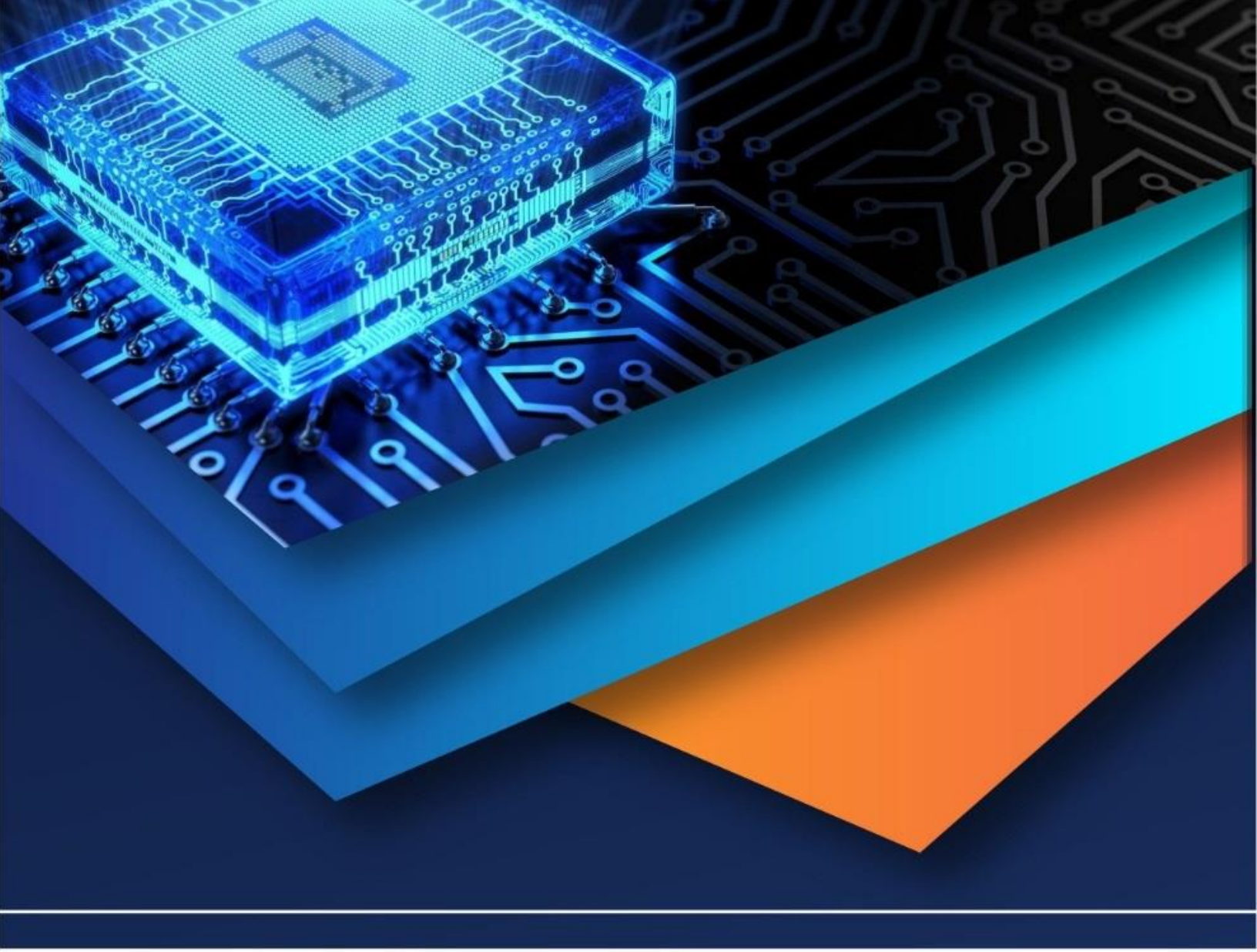

10.22214/IJRASET

45.98

IMPACT FACTOR: 7.129

IMPACT FACTOR: 7.429

# INTERNATIONAL JOURNAL FOR RESEARCH

IN APPLIED SCIENCE & ENGINEERING TECHNOLOGY